Available online at www.sciencedirect.com
SCIENCE DIRECT®
Journal of Power Sources 119–121 (2003) 934–937
JOURNAL OF POWER SOURCES
www.elsevier.com/locate/jpowsour

Effect of electrode density on cycle performance and irreversible capacity loss for natural graphite anode in lithium-ion batteries

Joongpyo Shim, Kathryn A. Striebel*

Environmental Energy Technologies Division, Lawrence Berkeley National Laboratory, Berkeley, CA 94720, USA

Abstract

The effect of electrode thickness and density for unpressed and pressed natural graphite electrodes were studied using electrochemical characterization. Pressing the graphite electrode decreased the reversible capacity and the irreversible capacity loss (ICL) during formation. As electrode density increased, the capacity retention at high rate increased until 0.9 g/cm^3, and then decreased. The cycle performances of the pressed graphite electrodes were more stable than the unpressed one. Pressing graphite electrode affected on its electrochemical characterization such as ICL, high rate cycling and cycle performance.

Keywords: Lithium-ion battery; Natural graphite; Anode

1. Introduction

Synthetic graphites, such as mesocarbon-microbead (MCMB) have been used commercially by many battery companies as anode materials in lithium-ion batteries because they have shown a reversible electrochemical behavior and a low, flat potential curve for the lithium intercalation/deintercalation process [1,2]. However, for all-electric and hybrid-electric vehicles, the lower-cost natural graphites are of more interest. Many approaches have been investigated for the stabilization of natural graphites to the point where the coulombic efficiencies approach that of the synthetics [3]. The dependence of the electrode preparation is critical to the performance of these materials. Recent reports on the relationships between the lithium intercalation process and pressure used during electrode preparation suggest that unpressed anodes yield superior performance due to faster kinetics and less disruption of the graphite morphology [4]. The dependence of SEI formation on anode density is far from solved. Some report a lower irreversible capacity loss (ICL) for more dense electrodes due to less exposed surface area [5]. For higher energy cells, it is clear from the patent literature and hearsay that pressing is a critical step in the production of high-performance anodes. In our search for a good anode for our low cost baseline EV cell technology, several different natural graphite materials were prepared and studied at different anode densities. We are investigating the dependence of the first-cycle ICL and cycling performance for different natural graphites on electrode loading and porosity.

Many factors influence the performance of graphite anodes. Type of graphite, including particle size, surface area, surface composition, and fraction of edge sites have all been shown to affect the charge of Li required to passivate the surface. Since this quantity of lithium directly affects the capacity of the cell, we are very interested in it. In addition, these factors can affect the stability of the anode layer. This translates to cell cyclability. Other electrode parameters such as layer porosity (or density) and binder content have also been studied. We have seen few reports dealing directly with the thickness (or capacity) of the anode layer. The dependence of anode density on the solid electrolyte interface (SEI) formation and cyclability is the subject of this work.

2. Experimental

The active materials used in this study are natural graphite (SL20, Superior Graphite Co.), 6% carbon-coated natural graphite (GDR6, Mitsui Mining Co.) and synthetic graphite (MAG-10, Hitachi Chemical). The anodes consisted of graphite (90–92%), PVdF binder (8–10%) and Cu foil current collector (thickness 25 μm). Slurries for electrode casting were prepared from a mixture of the graphite and

* Corresponding author. Tel.: +1-510-486-4385; fax: +1-510-486-7303.
E-mail address: kastriebel@lbl.gov (K.A. Striebel).

0378-7753/03/$ – see front matter © 2003 Published by Elsevier Science B.V.
doi:10.1016/S0378-7753(03)00235-0

PVdF dissolved in 1-methyl-2-pyrrolidinone (NMP). They were spread onto a Cu foil with different thickness and dried under vacuum at 120 °C for 12 h. After drying, the electrodes were compressed by bench top or roll press. All cells were assembled for testing in an Ar-filled glovebox.

Anodes were tested in two configurations: 30 mAh (12 cm^2) pouch lithium-ion cells prepared at LBNL from pressed and unpressed electrodes with 1 M $LiPF_6$/EC/DEC electrolyte and $LiCoO_2$ electrode. These pouch cells were cycled between 2.7 and 4.2 V with a taper charge at 4.2 V to a low-current cut-off of *C*/20. Electrodes (1 cm^2) were assembled into metal Swagelok cells with Celgard separator, electrolyte (1 M $LiPF_6$/EC/DEC) and Li foil reference/counter electrodes. Formation was carried out with two *C*/25 cycles and cycling was carried out with the same voltage limits at *C*/2. The voltage limits of 0.01–1.0 were used with a taper charge at 0.01 V (versus Li/Li^+).

3. Results and discussion

3.1. Formation

Fig. 1 shows the first and second cycles for natural graphite (SL20), synthetic graphite (MAG-10) and 6% carbon-coated natural graphite (GDR6) at *C*/25. Table 1 shows the reversible and irreversible capacities of these graphites for the formation cycle. SL20 and MAG-10 show lower ICL than GDR6 because the amorphous carbon black on the surface of GDR6 may induce the side reaction with the electrolyte. The reversible capacity of this SL20 natural graphite is very close to theoretical capacity.

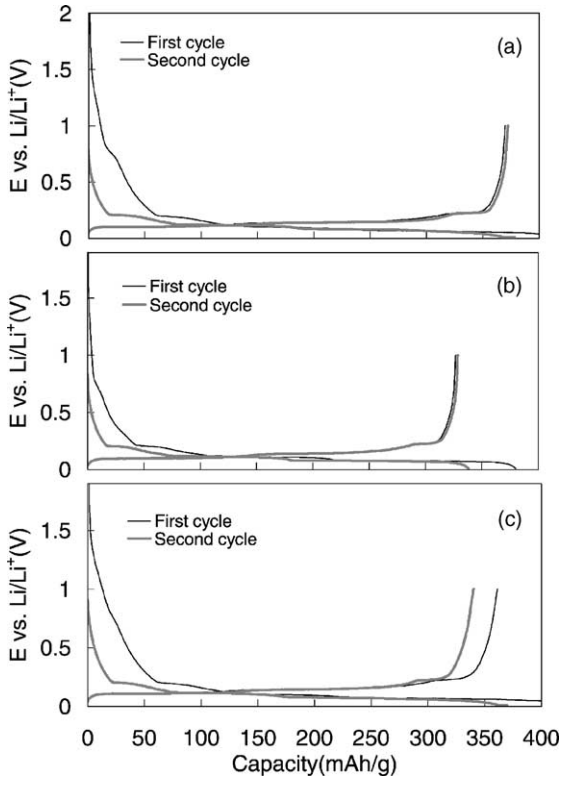

Fig. 1. First and second cycles of natural and synthetic graphites at *C*/25: (a) natural graphite (SL20); (b) synthetic graphite (MAG-10); (c) 6% carbon-coated natural graphite (GDR6).

Table 1
Reversible and irreversible capacities of natural and synthetic graphite for first and second cycles

Graphite	Q_{rev} (mAh/g)	ICL (%)	ICL (mAh/g)
SL20	370	9.2	75
MAG-10	328	8.6	62
GDR6	340	13.3	108

Fig. 2 shows the variation of electrode thickness and density for SL20 natural graphite on pressure with loading of 5.0 mg/cm^2. The electrode thickness decreased by pressing. The thickness reached to 50% of unpressed electrode around 300 kg/cm^2 and its density was 1.38 g/cm^3.

Fig. 3 shows the charge and discharge capacities of natural graphite anodes with different density for first and second cycles. The charge and discharge capacities decreased slightly with an increase of electrode density. The first charge capacities for all samples were over 400 mAh/g and reversible capacities at second cycle were around 360 mAh/g. Fig. 4 shows the total ICL for first and second cycles. ICL decreased slightly with an increase of electrode density. ICL for all electrode densities were 60–100 mAh/g and 8–12%. It has been reported that ICL comes from the side reaction between electrolyte and surface of graphite [6,7]. Zaghib et al. reported that the surface area of natural graphite was directly related to ICL regardless of particle size [8] but the reversible capacity was affected by the particle size of natural graphite [9]. If the electrode was compressed or rolled, the porosity and active surface area of electrode would be decreased. Also, the electrolyte volume in electrode and the contact area between electrolyte and graphite would be decreased. The result from Fig. 4 can be explained by those reasons.

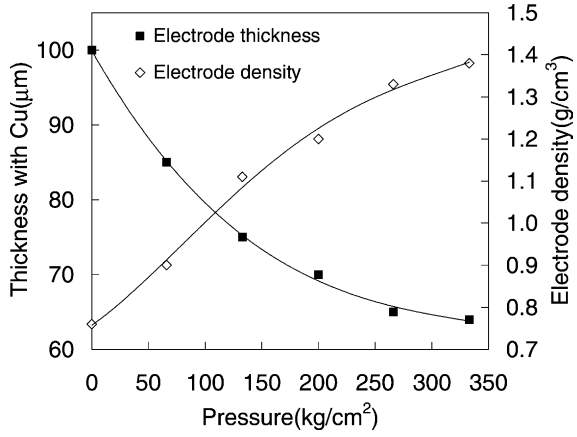

Fig. 2. Variation of electrode thickness and density for SL20 natural graphite by pressing: pressing time 5 s.

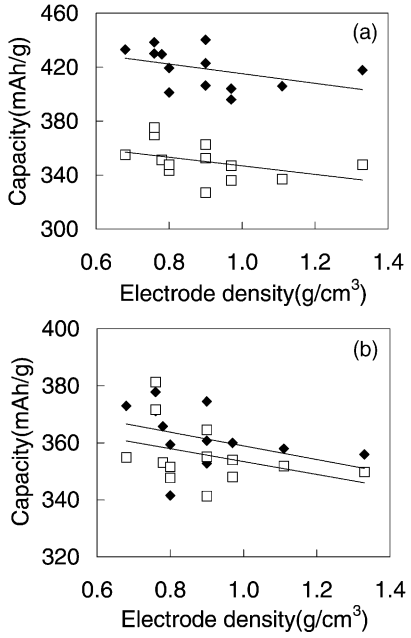

Fig. 3. Charge (filled symbols) and discharge (open symbols) capacities of unpressed and pressed graphite electrodes for first (a) and second (b) cycles.

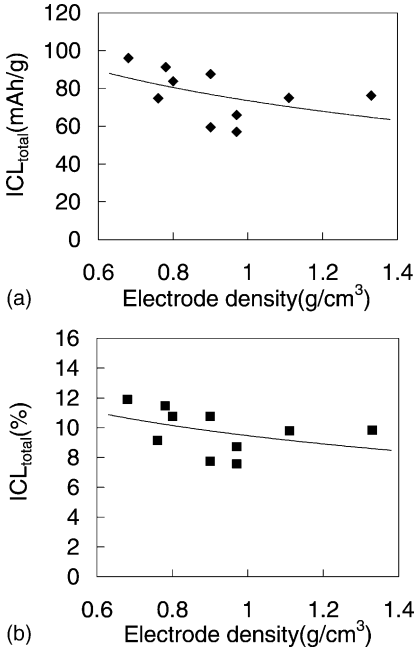

Fig. 4. Total ICL of natural graphite electrode for first (a) and second (b) cycles.

3.2. High rate utilization

Fig. 5 shows the voltage profiles for SL20 natural graphite with 0.9 g/cm^3 of electrode density at various C rates. Fig. 6 shows the variation of high rate capacity on electrode density at 3C. The graphite electrode around 0.9 g/cm^3 shows more than 90% of capacity retention at 3C rate. However, high rate

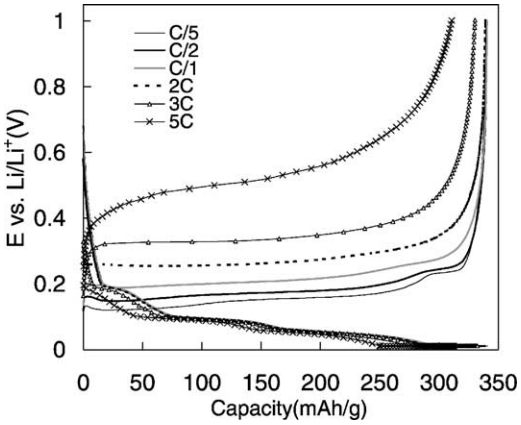

Fig. 5. Voltage profiles for SL20 natural graphite with 0.9 g/cm^3 of electrode density at various C rates: charge rate *C*/2.

capacity for the graphite electrode pressed to >1.0 g/cm^3 decreased. Highly pressed graphite electrodes showed lower capacity retention than unpressed electrode. Gnanraj et al. also reported that pressed graphite electrodes showed lower reversible capacity than unpressed ones [4]. They proposed that compressing graphite electrode might cause block the diffusion of lithium-ion into the active mass or damage them. But, their graphite electrode was subjected to higher pressures (a few ton per cm^2) than ours (in Fig. 2). Pressing of the natural graphite anodes increased electronic conductivity of the solid phase [10]. However, there will be a trade-off between decreasing ohmic resistance and ICL on the one hand and increasing polarization resistance of Li^+ transport in the electrolyte on the other, as porosity and thickness decrease. That will lead to a maximum. The role of electric conductivity in the performance of this electrode is the subject of future work.

3.3. Cyclability

Fig. 7 shows the discharge capacity during *C*/2 cycling for unpressed and pressed graphite electrodes in half-cell and pouch cell. Although the pouch cell with unpressed synthetic

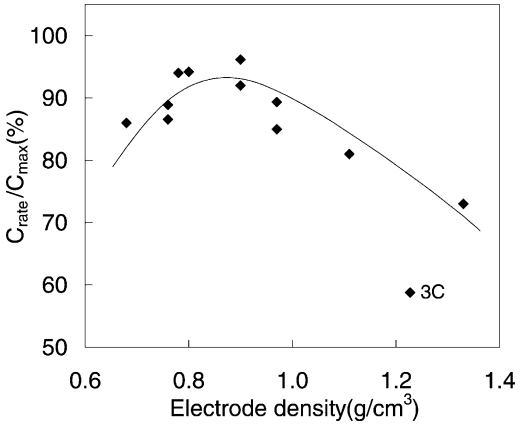

Fig. 6. Variation of high rate capacity on electrode density at 3C.

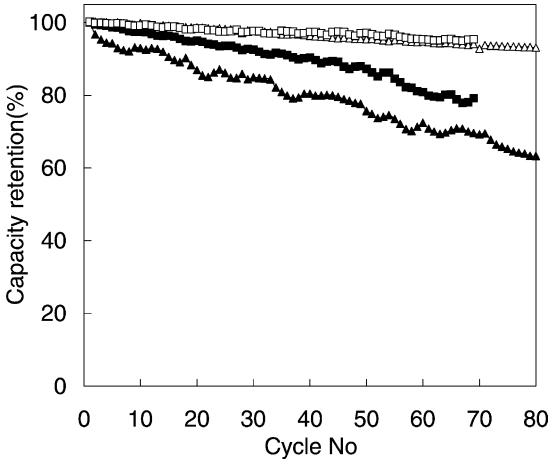

Fig. 7. Capacity retention for electrodes and cells with pressed (open symbols) and unpressed (filled symbols) electrodes: (△, ▲) pouch cell; (□, ■) natural graphite electrode.

graphite (density 0.51 g/cm^3) and $LiCoO_2$ electrodes showed rapid capacity fading, the capacity retention of that with pressed electrodes (1.11 g/cm^3 for anode) is very flat. We do not discuss the effect of pressing for cathode in this work. However, Gnanraj et al. have already reported the advantage for compressing cathode [4]. In half-cell test, the pressed natural graphite electrode (0.9 g/cm^3) showed better capacity retention than the unpressed one (0.76 g/cm^3).

When the composite electrode including active particle and binder is pressed, the porosity and thickness of electrode decrease and the stress for particles increases. If the porosity of electrode would be estimated by true density of graphite (2.26 g/cm^3) and PVdF (1.78 g/cm^3), it decreased from 65 to 40% before and after pressing. Active surface area in electrode decreases with a decrease of porosity. Although the electrode porosity by pressing decreased 60%, the capacity decreased 7–8% only in Fig. 3. A porosity of 40% is quite enough to allow electrolyte penetration into electrode. These results are consistent with the data of Novak et al. [11]. Manev et al. reported that there was optimum porosity for the performance of graphite electrode [12,13]. We also observed the optimum compacting pressure for high rate capacity and constant cycling, although it was lower than their data because of different pressing technique. Cycle performance and ICL are strongly affected by pressing electrode and these results are able to apply to battery production commercially.

4. Conclusion

The performance of natural graphite anodes on electrode density and porosity was investigated in 1 M $LiPF_6$/EC/DEC. The capacities of natural graphite electrodes for the first and second cycles decreased with an increase of electrode density by pressing. Also, pressed electrodes showed lower ICL than unpressed electrodes. The high rate utilization and cyclability of graphite electrode at moderate density of 0.9 g/cm^3 showed better performance than both unpressed (0.76 g/cm^3) and highly pressed (1.38 g/cm^3) electrodes. This result may be due to a trade-off between ohmic and polarization resistances in the porous electrode.

Acknowledgements

We acknowledge the supply of natural graphite from Superior Graphite Co. This research was funded by the Assistant Secretary for Energy Efficiency and Renewable Energy, Office of Advanced Automotive Technologies, US Department of Energy, under contract number DE-AC03-76SF00098.

References

[1] T. Nagaura, Prog. Batteries Battery Mater. 10 (1991) 218.
[2] T. Ohzuku, Y. Iwakoshi, K. Sawai, J. Electrochem. Soc. 140 (1993) 2490.
[3] H. Wang, M. Yoshio, J. Power Sources 101 (2001) 35.
[4] J.S. Gnanraj, Y.S. Cohen, M.D. Levi, D. Aurbach, J. Electroanal. Chem. 516 (2001) 89.
[5] K. Guerin, A. Fevrier-Bouvier, S. Flandrois, B. Simon, P. Biensan, Electrochim. Acta 45 (2000) 1607.
[6] D. Aurbach, A. Zaban, Y. Ein-Eli, I. Weissman, O. Chusid, B. Markovsky, M. Levi, E. Levi, A. Schechter, E. Granot, J. Electrochem. Soc. 68 (1997) 91.
[7] D. Aurbach, B. Markovsky, I. Weissman, E. Levi, Y. Ein-Eli, Electrochim. Acta 45 (1999) 67.
[8] K. Zaghib, G. Nadeau, K. Kinoshita, J. Electrochem. Soc. 147 (2000) 2110.
[9] K. Zaghib, F. Brochu, A. Guerfi, K. Kinoshita, J. Power Sources 103 (2001) 140.
[10] A.M. Sastry, BATT program quarterly report, Lawrence Berkeley National Laboratory, April 2002.
[11] P. Novak, W. Scheifele, M. Winter, O. Haas, J. Power Sources 68 (1997) 267.
[12] V. Manev, I. Naidenov, B. Puresheva, G. Pistoia, J. Power Sources 57 (1995) 133.
[13] V. Manev, I. Naidenov, B. Puresheva, P. Zlatilova, G. Pistoia, J. Power Sources 55 (1995) 211.